# Radar Transmitter Geolocation via Novel Observation Technique and Particle Swarm Optimization

**John G. Warner**
**US Naval Research Laboratory**
**Washington, DC 20375**
**202-279-5060**

**Jay W. Middour**
**US Naval Research Laboratory**
**Washington, DC 20375**
**202-279-4338**

*Abstract*— **The ability to precisely determine the location of radar transmitters can be crucially important in maintaining domain awareness. This, however, may be problematic with traditional methods when used with a distributed network of disparate sensors. A novel geolocation technique for circularly scanning radar transmitters is introduced. This technique uses the differenced central times of arrival (DCTOA) of the main beam as an observable. The solution for the transmitter's position and scan rate are given using a weighted least squares approach as well as a particle swarm optimizer. Experimental results show this technique is able to locate a radar transmitter within 11 meters, while maintaining minimal complexity. This technique has the advantage of requiring orders of magnitude less timing synchronization among receivers, an order of magnitude less data transfer, and it does not require simultaneous illumination of receivers.**

## TABLE OF CONTENTS



## 1. INTRODUCTION

The ability to accurately locate radar sources in a timely manner is crucial in maintaining maritime and other domain awareness. Traditional methods of precision geolocation require multiple receivers to be time synchronized on the order of nanoseconds and often require simultaneous illumination. Further, receivers must exchange data that often occurs at the pulse rate of the radar. This, however, may present a challenge when a distributed network of diverse sensors is used that have limited timing and data exchange abilities. A method of precision geolocation with less stringent timing and data exchange requirements would enable a disparate network of sensors to accurately estimate a radar transmitter's location, as well as expand the state of the art of radar geolocation techniques.

There are a number of methods currently used for radar geolocation. Reference [1] provides a general survey of techniques, while Reference [2] discusses the theory of these techniques in detail. Many of these techniques require the same radar signal to be observed by multiple receivers. A common example of this is Time Difference of Arrival (TDOA), where the difference in signal time of arrival is measured between two spatially distributed receivers. Details of this technique can be found in Reference [3]. This technique may be problematic with arbitrarily distributed receivers as it requires simultaneous illumination and precise timing synchronization between receivers (as solution error is proportional to timing error times the speed of light). Other common techniques have similar requirements but observe different signal characteristics. For example, the difference in the phase of the signal between two receivers may be observed in interferometry or the Difference in the Frequency of Arrival (FDOA) may be used to estimate a radar transmitter's location. These techniques have similar timing constraints and will further require data to be shared between receivers at the pulse rate of the radar, which may be prohibitive.

Additionally, the doppler shift of the signal may be observed, if there is relative motion between the transmitter and the receiver, and can be used to estimate a transmitter's location. This technique may be problematic in practice as it generally requires information about the emitted frequency, which may not be readily available and may vary over time in an unknown fashion. Reference [4] contains further discussion of this method.

The last common technique is based on the Angle of Arrival (AOA) of the signal. Reference [5] as well as Reference [2] give ample discussion of this method. This technique uses multiple measurements of the AOA of a signal to triangulate its source. This method does not require precision timing synchronization of receivers or high rates of data exchange. However, as determining the AOA of a signal to sufficient accuracy may be challenging, precise geolocation results are not often achievable.

A novel method has been developed that uses differenced times of arrival of maximum signal strength across multiple receivers to locate a circularly scanning radar transmitter. The method allows for passive, precision geolocation without precise timing requirements or prohibitive data exchange volumes. The difference between signal times of arrival is related to the angle the radar has swept out between observation events, thus the radar transmitter location may be calculated to be along a line of constant angle between the two receivers. Given sufficient data, the radar transmitter's location may be estimated. This method has the advantage of being independent of platform and tolerant to timing error on the order of hundreds of microseconds.

This technique has been developed and tested at the US Naval Research Laboratory (NRL), and has been developed by other


[1] IEEEAC Paper #1582, Version 1.0, Updated 21/12/2011.

researchers in References [6], [7] and [8]. Major work at NRL include field tests in 2006 and 2009, the latter of which is documented in Reference [9]. NRL has been issued a United States patent for this algorithm, [10].

A complete description of the methods used to reliably implement this technique, called SearchLight, are presented. The development of the basic observable is presented along with the necessary algorithm to allow the technique to be used for an arbitrary receiver configuration. Next, methods for estimating the radar transmitter's position are presented for both the linearized and the nonlinear system. The nonlinear optimization process has the added benefit of being able to easily resolve a location ambiguity that exists within the system. Last, experimental results are presented using data from the 2009 data collection. Ultimately, it is shown that the SearchLight algorithm enables precision radar geolocation using distributed receivers without the need for precise timing synchronization.

## 2. THE SEARCHLIGHT METHOD

The SearchLight concept makes use of the fact that a stationary, circularly scanning radar transmitter will illuminate a receiver at a regular interval. If one envisions two receivers distributed about a circularly scanning radar, the change in time of illumination between the receivers is equal to the angle the transmitter sweeps out between the receivers divided by the scan rate of the transmitter. This can be expressed by the following equation.

$$t_j - t_i = \frac{1}{\omega} \cos^{-1}\left(\frac{(\boldsymbol{r}_i - \boldsymbol{r}) \cdot (\boldsymbol{r}_j - \boldsymbol{r})}{|\boldsymbol{r}_i - \boldsymbol{r}|\,|\boldsymbol{r}_j - \boldsymbol{r}|}\right) \tag{1}$$

In practice, the position of the transmitter, given here by $\mathbf{r}$, is the unknown quantity that must be derived along with the scan rate, $\omega$, given a series of differenced central times of arrival (DCTOA), $t_i$ and positions at these times, $\boldsymbol{r}_i$. While the position vector may be expressed in either a local vertical local horizontal coordinate system or in an Earth fixed coordinate system, the implicit assumption is that the radar transmitters and receivers do not vary significantly from the local tangent plane. The central time of arrival for a receiver is defined as the time of arrival of maximum signal amplitude (corresponding to the arrival of the center of the main radar beam).

The method for determining the central time of arrival is dependent on radar signal characteristics as well as the number of active radar in the collection area. When there are multiple active radar being collected against, each signal must be deinterleaved. There are several methods for accomplishing this, all of which rely on the specific characteristics of the radar to properly sort the signals. Reference [2] contains a general overview of available techniques. Once each radar signal has been isolated, the central time of arrival may be calculated. For pulsed radar, this time may be estimated by fitting a quadratic curve to the center of received radar pulses and calculating the time corresponding peak of the quadratic for each radar pass. A similar technique may be applied to continuous wave radar.

It should be noted that the angle calculated in Equation 1 is by definition of *arc cosine* between 0 and $\pi$; therefore, a check is necessary not only to ensure the correct quadrant is resolved, but also that the calculated angle between receivers is indeed the angle the radar has swept out between detection events.

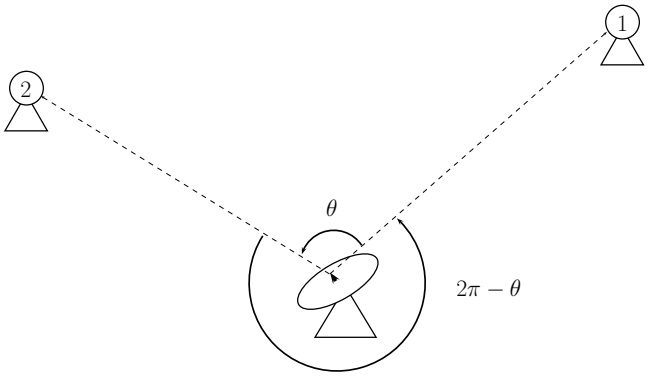


**Figure 1**. Diagram Showing Example of Relative Geometry of Two Fixed Receivers to One Fixed Radar Transmitter

Consider Figure 1. As the radar transmitter sweeps in a counter-clockwise direction, the angle it sweeps between consecutive receiver illumination events will alternate between $\theta$ and $2\pi - \theta$. That is, the angle that the radar transmitter sweeps from receiver one to receiver two is $\theta$, while the angle the transmitter sweeps from receiver two to receiver one is $2\pi - \theta$. However, the *calculated* angle between the receivers will always remain $\theta$. A set of geometric checks must be implemented to differentiate these cases in order to calculate the correct error residual and to extend this technique to arbitrary receiver geometry.

It can be shown that angle the radar sweeps between detection events falls into one of three cases. As shown above, the first case occurs when the radar has swept out exactly the calculated angle $\theta$ between detection events. In the next case, the radar has swept out not $\theta$ but its explement (i.e. $2\pi - \theta$). These cases are demonstrated in Figure 1. The last possible case occurs for one mobile receiver. Between detection events, the receiver may have displaced an angle $\theta$ with respect to itself. In this case, the radar sweeps out one complete revolution plus the additional angular displacement, which is $2\pi + \theta$. This occurs when the receiver moves with the direction of radar sweep: when the receiver moves against the radar sweep the angle is $2\pi - \theta$. Assuming that system uncertainty is small with respect to the time between detection events, the correct DCTOA error residual is implemented as the following.

$$\theta = \cos^{-1}\left(\frac{(\boldsymbol{r}_i - \boldsymbol{r}) \cdot (\boldsymbol{r}_{i+1} - \boldsymbol{r})}{|\boldsymbol{r}_i - \boldsymbol{r}|\,|\boldsymbol{r}_{i+1} - \boldsymbol{r}|}\right) \tag{2}$$

$$e = \text{DCTOA}_{observed} - \text{DCTOA}_{computed} \tag{3}$$

$$= \min \begin{bmatrix} \text{DCTOA}_{observed} - \theta/\omega \\ \text{DCTOA}_{observed} - (2\pi - \theta)/\omega \\ \text{DCTOA}_{observed} - (2\pi + \theta)/\omega \end{bmatrix} \tag{4}$$

To reiterate, for each measurement a calculated difference central time of arrival will be computed based on the current estimate of the radar transmitter's position and scan rate. This calculated DCTOA must be checked against the observed DCTOA to ensure that the correct geometric case is identified. From here, the error residual is computed as the value that is the minimum of the three geometric cases discussed above and shown in Equation 4. This method is valid as measurement error is at least an order of magnitude lower than time difference between the three geometrical

cases. It should be noted that without making this correction, the algorithm is constrained to geometric cases where each receiver is $180^o$ or less apart from each other with respect to the radar transmitter.

Note that this relationship holds true regardless of receiver configuration. The benefit of this method is that data from any number of receivers in any distribution may be used to estimate the radar transmitter's location without additional impact upon the SearchLight algorithm. Indeed, the only requirement is that sufficient change in receiver bearing with respect to the transmitter is observed; thus, a multitude of receiver platforms and configurations are supported.

Further, it can be seen that information regarding specific transmitter characteristics is not necessary *a priori*. This gives SearchLight an advantage of competing geolocation techniques such as geolocation via doppler shift observation, where the emitted signal frequency must be known. Also, only the arrival of the center of the main radar beam must be isolated when multiple transmitters are present, rather than the arrival of each pulse. This may decrease the complexity in the signal deinterleaving process and allow the SearchLight algorithm to be used in applications where specific signal characteristics are not known *a priori*.

Next, SearchLight may be used to geolocate Continuous Wave (CW) radar transmitters. Many traditional techniques, such as TDOA, use the arrival of pulses to define a measurement event and cannot be easily implemented to geolocate CW radar transmitters.

Last, it can be seen from Equation 1 that this observation is much less sensitive to clock error than traditional time difference of arrival (TDOA) methods. In TDOA methods, the resulting position error due to clock error is proportional to the speed or light; however, for this DCTOA method, the position error is only proportional to the scan rate of the radar transmitter, which is several orders of magnitude slower. Thus, much larger clock errors are tolerable. This fact enables this method to be used with distributed receivers without the need for precise timing calibration. Additionally, the requirements for data transfer with this algorithm is much lower than traditional methods. Traditional techniques require data measurements to be taken at the pulse rate of the radar, while this technique only requires the sharing of data taken at the scan rate of the radar transmitter. This typically results in the need for one order of magnitude less data transfer between receivers to formulate a geolocation solution.

## 3. SOLVING THE LINEARIZED SYSTEM

Given multiple DCTOA measurements, a stationary, circularly scanning radar transmitter's position and scan rate may be estimated. It is clear that the measurement equation (Equation 1) is nonlinear, so a linearized least squares solution may be used. The least squares criteria was first posed by Gauss. For a more in depth treatment see References [11] or [12]. Here the state that is solved for is the radar transmitter's position, $\mathbf{r}$, and scan rate, $\omega$. The measurement is the DCTOA, which is related to the state by Equation 1, which is repeated for completeness.

$$\boldsymbol{x} = \begin{bmatrix} \boldsymbol{r} \\ \omega \end{bmatrix} \tag{5}$$

$$\boldsymbol{y} = \frac{1}{\omega} \cos^{-1}\left( \frac{(\boldsymbol{r}_i - \boldsymbol{r}) \cdot (\boldsymbol{r}_{i+1} - \boldsymbol{r})}{|\boldsymbol{r}_i - \boldsymbol{r}|\,|\boldsymbol{r}_{i+1} - \boldsymbol{r}|} \right) \tag{6}$$

$$= h(\boldsymbol{x}, \boldsymbol{r}_i, \boldsymbol{r}_{i+1}) \tag{7}$$

To linearize the measurement equation, the first order variation of its Taylor series expansion about a known constant state $\boldsymbol{x_0}$can be considered. So then, the following equations hold.

$$\tilde{\boldsymbol{y}} = h(\boldsymbol{x}, \boldsymbol{r}_i, \boldsymbol{r}_{i+1}) - h(\boldsymbol{x_0}, \boldsymbol{r}_i, \boldsymbol{r}_{i+1}) \tag{8}$$

$$\tilde{\boldsymbol{y}} \approx H\left[\boldsymbol{x} - \boldsymbol{x_0}\right] \tag{9}$$

$$H = \frac{\partial h(\boldsymbol{x}, \boldsymbol{r}_i, \boldsymbol{r}_{i+1})}{\partial \boldsymbol{x}} \tag{10}$$

In the weighted least squares (WLS) formulation the goal is to estimate the state, $\boldsymbol{x^o}$, that minimizes the following cost functional, which is the sum of the squares of the error.

$$J(\boldsymbol{x}) = 1/2\, \boldsymbol{\epsilon}^T W \boldsymbol{\epsilon} \tag{11}$$

$$= 1/2\, \left(\tilde{\boldsymbol{y}} - H\boldsymbol{x}\right)^T W \left(\tilde{\boldsymbol{y}} - H\boldsymbol{x}\right) \tag{12}$$

Here, $W$ is a positive definite weighting matrix which is generally set to the inverse of the measurement noise covariance. This has the well-known solution shown below.

$$\boldsymbol{x}^o = \left(H^T W H\right)^{-1} H^T W \tilde{\boldsymbol{y}} \tag{13}$$

This quantity is often described in terms of the covariance matrix, $P$.

$$P = \left(H^T W H\right)^{-1} \tag{14}$$

$$\boldsymbol{x}^o = P H^T W \tilde{\boldsymbol{y}} \tag{15}$$

As this is a nonlinear WLS problem, an initial state estimate,$\boldsymbol{x_0}$, must be generated and the solution must be iterated upon until convergence. An initial guess for the radar transmitter's position can be generated by a rough grid search. To generate an initial guess on the radar's scan rate, the times between detection events for any individual receiver can be averaged. This may then be averaged between all receivers. This time divided by $2\pi$ yields a fairly accurate guess of scan rate. This is because the time between detection events for each individual receiver roughly corresponds to one complete revolution of the radar beam.

While an analytic form of the matrix $H$ may be found (this is shown in the Appendix), analysis has shown that calculating numerical partial derivatives generally yield better results. Reference [8] contains an alternate formulation of this solution.

## 4. SOLVING THE NONLINEAR SYSTEM

As the system is nonlinear, it would be beneficial to estimate the radar transmitter's position and scan rate in a nonlinear fashion. Additionally, there is an issue that makes nonlinear analysis preferable. It can be seen from Equation 1 that any given DCTOA can be generated by estimating the radar transmitter at the true position and true scan direction or at a position mirrored about the line joining the measurement locations and having the opposite scan direction. This false location will be referred to as a "ghost point." This ghost point will move as the relative geometry of the receivers change; however, the area in the vicinity of the ghost point will represent a local minimum of the sum of the squared error. This may cause the WLS to erroneously converge. Thus, a method for locating a global minimum (despite the existence of local minimums) is necessary. An example of this phenomenon can be seen in Figure 2 below. As can be seen, there is a distinct local minimum corresponding to the ghost point mirrored about the mobile receiver position.

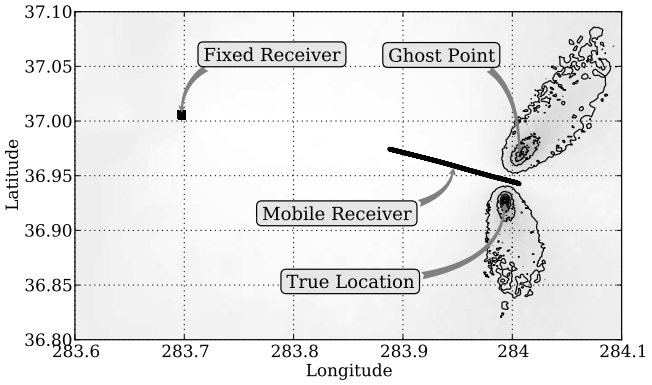


**Figure 2**. Plot Showing Error Contours of the Cost Function with Relative Receiver Geometery for F1 Dataset

In order to meet these goals, a particle swarm optimizer (PSO) was implemented. PSO was first theorized in References [13] and [14]. For a more in depth discussion see Reference [15], while Reference [16] provides an excellent overview of the process. The problem must be posed as finding a minimal value of a cost function given a set of input parameters. This applies exactly to the SearchLight problem: the sum of the squares of the residuals may be minimized by finding the correct transmitter location and scan rate. From here, the search space for the solution must be defined. In terms of this application, this means that appropriate bounds need to be placed on the location as well as the scan rate for the receiver. In this execution of the PSO, the initial bounds on the radar transmitter's position have been as large as two degrees in latitude and longitude. The initial bounds on the scan rate can either be estimated by the end user or taken as within a reasonable percentage of the estimated scan rate using the method described above. Next, the search space is randomly populated with a number of state guesses (in this case receiver position and scan rate), known as particles. These particles are also given an arbitrary initial velocity. At each time step the cost function is evaluated for each particle, and the a number of best states are tracked. The first tracked state is known as the individual best solution which corresponds to state with the lowest cost at any time step on a strictly per particle basis. So, for $N$ particles, there will be $N$ individual best states tracked. The next tracked state is known as the global best solution and is the state with the lowest cost for any particle at any time step. There is typically only one global best solution. From here, each particle is stochastically accelerated along three directions: along its current direction, towards its best known individual solution and towards the best known global solution. This process is iterated until a stopping condition is met, which is typically a fixed number of iterations.

The equations in this process are defined in the following paragraphs. Here, the objective function is defined as the sum of the squares of the residual error: this is a function of transmitter position and transmitter scan rate.

$$J(\boldsymbol{x}) = \sum_{i=2}^{N} (y^i - h^i(\boldsymbol{x}, \boldsymbol{r}_{i-1}, \boldsymbol{r}_i))^2 \tag{16}$$

Here, $y^i$ and $h(\boldsymbol{x}, \boldsymbol{r}_i, \boldsymbol{r}_{i+1})^i$ are the $i^{th}$ observed DCTOA and calculated (via Equation 1 and Equation 4) DCTOA, which are summed over $M$ observations.

Now, an initial population of particles can be created. This is done by uniformly, randomly populating the search space with $N$ number of initial states. This is accomplished by invoking the following equation for the $j^{th}$ particle.

$$\boldsymbol{X}_j = \boldsymbol{X}_{min} + r(0,1)\,\boldsymbol{d} \tag{17}$$

$$\boldsymbol{d} = \boldsymbol{X}_{max} - \boldsymbol{X}_{min} \tag{18}$$

$\boldsymbol{X}_j$ is the state of the $j^{th}$ particle, $\boldsymbol{X}_{max}$ is the upper bound of the search space, $\boldsymbol{X}_{min}$ is the lower bound for the search space and $r(0,1)$ signifies a random number with uniform distribution between 0 and 1.

The following process is then iterated until a suitable stopping condition is reached. First, evaluate the objective function for each particle.

$$\Upsilon_j = J(\boldsymbol{X}_j) \tag{19}$$

Next, check to see if this current state represents either an individual best solution for the $j^{th}$ particle, denoted by $\boldsymbol{\psi}_j$, or a global best solution, represented by $\boldsymbol{G}$. Here, only one global best solution will be tracked. If these conditions are satisfied then the following are implemented.

$$\boldsymbol{\psi}_j = \boldsymbol{X}_j \qquad \text{if } \Upsilon_j < J(\boldsymbol{\psi}_j) \tag{20}$$

$$\boldsymbol{G} = \boldsymbol{X}_j \qquad \text{if } \Upsilon_j < J(\boldsymbol{G}) \tag{21}$$

For $M$ particles, the algorithm tracks $M$ individual particle best solutions and typically one global best solution. The individual and global best solutions are not necessarily updated at every iteration; rather, they are only updated when a better individual particle solution or global solution is found. This is known as a global best topology. A formulation can be made where each particle is only aware of the best solution within its group of neighbors as defined in state space, as opposed to each particle having knowledge of best solution globally. This formulation is generally regarded as allowing the PSO to be more resistant to premature convergence; however, it requires more computation and was not deemed necessary for this work. Further discussion is available in Reference [17].

Now that all particles have been evaluated and checked for the individual or global best solutions, the particles must be moved to a new position for the next iteration. This is

accomplished in the following manner. First, the velocity of each particle is set in the following manner.

$$\begin{aligned} \boldsymbol{V}_j^k = \; & c_I \;\; \boldsymbol{V}_j^{k-1} \\ & + c_C \left( \boldsymbol{\psi}^k - \boldsymbol{X}_j^{k-1} \right) \\ & + c_S \left( \boldsymbol{G} - \boldsymbol{X}_j^{k-1} \right) \end{aligned} \tag{22}$$

Here, $j$ refers to the $j_{th}$ particle and $k$ refers to the $k_{th}$ iteration. The initial particle velocity can be assigned arbitrarily. In this implementation, the velocity direction was randomly assigned while the magnitude was set to be arbitrarily small. As can been seen, the particle's velocity is impacted by three main factors: the particle's previous velocity, the vector difference between its individual best state and its current state, and the vector difference between the globally best solution and its current state. These three quantities are scaled by inertial, $c_I$, cognitive, $c_C$ and social, $c_S$ weights, which are defined in the following manner.

$$\begin{aligned} c_I &= \frac{1 + r_1(0,1)}{2} \\ c_C &= 1.49445\, r_2(0,1) \\ c_S &= 1.49445\, r_3(0,1) \end{aligned} \tag{23}$$

Notice each of these three constants involve an independent uniform random number, given by $r_i(0,1)$. Each of these stochastic scale factors were chosen from suggested values in the literature and may be adjusted in a number of ways. Both References [18] and [19] discuss the effects of altering these parameters. Once the particle velocity is calculated, the particle is propagated to its new location in the following manner.

$$\boldsymbol{X}_{j+1}^i = \boldsymbol{X}_j^i + \boldsymbol{V}_j^i \tag{24}$$

This then concludes one iteration. This process is then repeated until an appropriate stopping condition is met.

## 5. CONFIDENCE REGION CALCULATION

In many applications, it is not sufficient to only estimate the position of the radar transmitter: it is necessary to estimate the size of the confidence region about the solution. There are two methods that were explored.

First, a confidence ellipse may be calculated from the linearized system. Reference [20] gives an excellent review of calculating a confidence ellipse given a covariance matrix. The covariance matrix, $P$, of the linearized system is related to the confidence ellipse through its eigenvalues, $\lambda_i$, and eigenvectors, $\boldsymbol{v}^i$. As the primary concern is for the uncertainty in the radar transmitter's position, consider the reduced two by two covariance matrix, $P_{2x2}$ (which corresponds to the position covariance), and let its eigenvalues be $\lambda_1 > \lambda_2$. The confidence ellipse can be defined by its semi-major axis, $SMA$, its semi-minor axis, $SMI$, and its orientation angle, $\phi$. These are defined by the following.

$$SMA = \sqrt{2\lambda_1 \sigma^2 F_{p,n-p}^{1-\alpha}} \tag{25}$$

$$SMI = \sqrt{2\lambda_2 \sigma^2 F_{p,n-p}^{1-\alpha}} \tag{26}$$

Here, $\sigma^2$ represents the calculated error variance, $F$ represents the percentage point of the Fisher distribution, $\alpha$ represents the confidence level, $p$ is the number of degrees of freedom and $n$ is the number of data points. The Fisher distribution is itself a ratio of Gamma function and generally has numerical values available in standard math tables. The orientation of the ellipse can defined as the angle of the first eigenvector (i.e. the direction of the semi-major axis) with respect to the first coordinate axis. This is given by the following.

$$\phi = \arctan\left( \frac{v_2^1}{v_1^1} \right) \tag{27}$$

Here, $v_l^1$ represents the $l^{th}$ component of the first eigenvector. This method has the advantage of being well suited to a WLS approach as the covariance is already calculated. However, it makes the assumption that the confidence ellipse is centered upon the solution position, which is not necessarily the case. Additionally, the ellipse is derived from the covariance of the linearized system, which may not yield the correct result in a nonlinear system.

Thus, a nonlinear method for developing the confidence region is needed. References [21] and [22] both discuss several methods for developing a confidence region in the context of PSO. A general confidence region can be expressed by the formula for the likelihood method which is as follows.

$$J(\boldsymbol{x}) - J(\boldsymbol{x^o}) \leq \sigma^2 p F_{p,n-p}^{1-\alpha} \tag{28}$$

This equation, which was first formalized in Reference [23], states the confidence region is the locus of points $\boldsymbol{x}$ in state-space such that the difference between the cost function at that point and the cost function at the optimal point $\boldsymbol{x^0}$ is within a constant, which itself is a function of the error variance, degrees of freedom and the associated percentage point of the Fisher distribution.

This definition of a confidence region lends itself well to the PSO process. A key feature of PSO is the evaluation of the cost functional at a large sampling of points. Thus, a byproduct of this is the ability to evaluate whether a point satisfies Equation 28, and thereby create the locus of points that represents the confidence region.

This process is implemented in several steps. First, within the PSO algorithm a check can be added for each particle as to whether it satisfies Equation 28. If it is satisfied, the point and value of the cost function are stored for post processing. After the PSO has run to completion, a check must be run to ensure each point that has previously satisfied Equation 28 still indeed satisfies the equation (as the value of the optimal cost has no doubt been updated throughout each iteration). The remaining set of points represents the nonlinear confidence region. A set of points, however, is difficult to express by a few meaningful quantities. Thus, it was decided that the minimum volume containing ellipse (MVCE) should be fit to these points so that the size and orientation of region may be expressed in identical terms as in the linearized confidence region. In order to make this process more efficient, the convex hull of this set of points

may be found before calculating the MVCE (since the MVCE of a set of points is identical to the MVCE of its convex hull). The convex hull is defined as the minimum subset of points such that all points are contained within them.

This process has a few benefits derived from the fact that the confidence region is explicitly linked to the evaluation of the cost functional. First, this method is able to identify when a cost minimum represented by the ghost point is within the confidence region of the true minimum. This can be a quality measure by the end user to determine whether sufficient data has been taken to definitively locate the radar transmitter. An additional benefit of this method is that the ellipse is not assumed to be centered upon the optimal solution. This fact can aid in identifying modeling problems by more readily distinguishing when the true solution does not lie within the confidence region in excess of what is statistically predicted.

## 6. TESTING RESULTS

An exercise was conducted where a fixed receiver and a moving, ship-based, mobile receiver were collecting data while in range of three separate radar transmitters to test these methods. These transmitters had varied characteristics. These receivers collected a synchronized time tag, their own position as well as radar data. The relative geometries of the radar transmitters and the receivers are shown in Figure 3 below.

As can be seen, the fixed radar transmitters were installed in a coastal location. The ship-board receiver traveled along the coast so that the effects of relative geometries could be observed. Figure 3 also shows how the data have been divided into subsets, each set ranging from 10 to 30 minutes of collection time.

Both the WLS method and the PSO algorithm were implemented on the dataset. The estimated radar position was compared against the known position for each data segment. The results of this analysis are summarized in Table 1 below. As an additional point of comparison, data for a line of bearing (LOB) geolocation process was simulated. The technique uses the angle of arrival (AOA) of the signal and essentially uses triangulation to determine the radar transmitter's location. References [2] and [5] contain detailed discussion of this method. This was done so that an appropriate comparison can be made, as the LOB technique also does not require precision time synchronization and may be used with distributed receivers. Both the WLS and LOB results are taken from Reference [9] to serve as a point of comparison against the PSO results.

As can be seen the SearchLight algorithm provides geolocation results with much higher accuracy than the line of bearing method. The positions calculated via the SearchLight algorithm are on average twenty times more accurate.

Furthermore, it is clear that the PSO generally provides more accurate results than the WLS method. The average miss distance is almost 150 meters lower for the PSO method. In addition to the more accurate results, the PSO method requires much less data preprocessing than the WLS method. The WLS requires not only an initial guess for the radar transmitter's position and scan rate, but it also requires more data checking to ensure that it will not converge to the ghost point. The PSO method, on the other hand, requires only a rough search space definition and is able to uniformly process data with little intervention. And since the WLS method requires additional preprocessing, the run times for both methods are comparable, even though a PSO is traditionally more computationally intensive.

**Table 1**. Data Analysis Results Summary of Miss Distances in Meters[2]

| Dataset | PSO Method | WLS Method | LOB Method |
|---|---|---|---|
| F1 | 11.0 | 9.3 | 926.0 |
| F2 | 38.5 | 53.7 | 1296.4 |
| F3 | 199.2 | 398.2 | 6667.2 |
| F4 | 80.4 | 196.3 | 2592.8 |
| F5 | 160.1 | 368.5 | 7408.0 |
| F6 | 72.8 | 561.2 | 14630.8 |
| F7 | 667.0 | 822.3 | 11112.0 |
| L1 | 72.1 | 20.4 | 1296.4 |
| L2 | 45.3 | 131.5 | 9074.8 |
| N1 | 136.5 | 785.2 | 1852.0 |
| N2 | 732.3 | 724.1 | 1481.6 |
| N3 | 550.9 | 492.6 | 2963.2 |
| **Min** | 11.0 | 9.3 | 926.0 |
| **Max** | 732.3 | 822.3 | 14630.8 |
| **Avg** | 230.5 | 380.3 | 5108.4 |

Next, the confidence region of these solutions can be calculated from both the linearized and nonlinear methods. These regions can be constructed for a given confidence level (e.g. 95%) and represent where the estimated solution may lie if more or varied data is used to compute the solution. It should be noted that this does not necessarily mean that the true solution will lie within the confidence region at that given probability.

Confidence ellipses were calculated at a 99.9% confidence level in both the linearized and nonlinear method as described above for each dataset. It was also noted whether the confidence region contained the true solution or not. These results are presented in Table 2 below.

It can be seen from those results that nonlinear method provides confidence regions that are much smaller, but only contain the solution for half of the cases while the linearized solution provides confidence regions that are much larger but contain the true solution for all datasets. At this chosen confidence level, it would be expected that each confidence region would approximately always contain the true solution if the system is correctly modeled. This indicates that system modeling can be improved. Indeed, upon examination of a contour plot of the error residuals, it can be seen that the true solution is not located within a minimum error residual location.

A plot of the results for dataset F1 are shown below in Figure 4. As can be seen, the estimated radar transmitter location is within 11 meters of the true transmitter location. The 99.9% nonlinear confidence ellipse is plotted as well for a point of reference. Figure 5 shows a plot of the results for the F3 dataset. These results show the case where the true solution is not contained within the confidence ellipse. It should be

[2]WLS and LOB results are from [9]

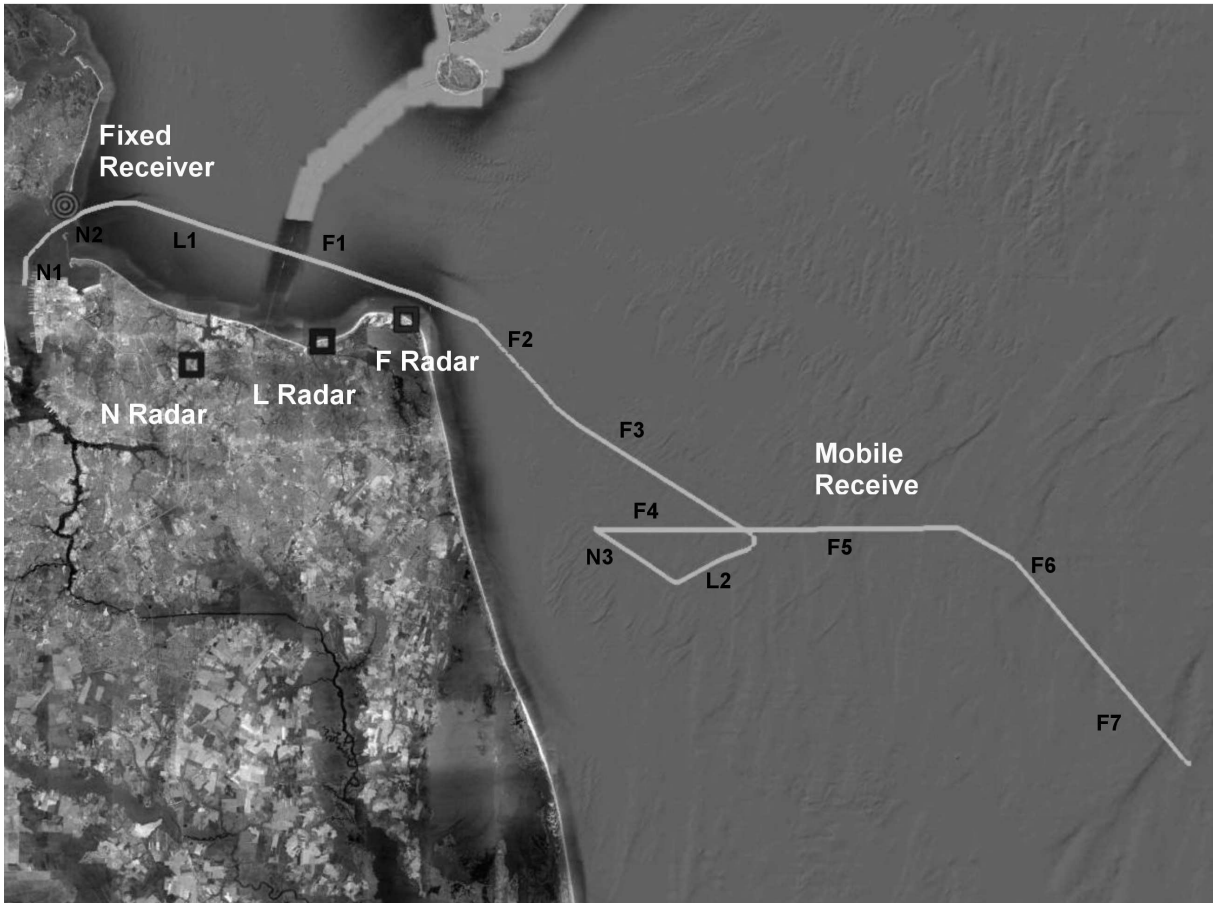


**Figure 3**. Plot Showing Relative Positions of Radar Transmitters Versus Receivers Over Collection Period

**Table 2**. Results Summary for Confidence Region Analysis

| | *Nonlinear Method* | | | *Linearized Method* | | |
|---|---|---|---|---|---|---|
| **Dataset** | **SMA [m]** | **SMI [m]** | **Contained** | **SMA [m]** | **SMI [m]** | **Contained** |
| F1 | 332.10 | 163.34 | In | 288.81 | 139.45 | In |
| F2 | 93.09 | 20.36 | Out | 274.02 | 57.37 | In |
| F3 | 1286.39 | 28.64 | Out | 7380.09 | 80.43 | In |
| F4 | 313.16 | 22.11 | Out | 1660.67 | 80.14 | In |
| F5 | 570.94 | 28.49 | Out | 4470.12 | 99.37 | In |
| F6 | 2635.31 | 45.32 | Out | 21014.90 | 138.75 | In |
| F7 | 5259.61 | 126.09 | In | 50190.45 | 315.56 | In |
| L1 | 1872.81 | 202.33 | In | 3584.14 | 367.26 | In |
| L2 | 1749.42 | 116.66 | In | 7644.55 | 216.75 | In |
| N1 | 19217.66 | 1988.07 | In | 24307.59 | 345.76 | In |
| N2 | 349.64 | 155.37 | Out | 1200.12 | 508.43 | In |
| N3 | 7769.74 | 6073.10 | In | 30136.18 | 72.13 | In |

noted that the confidence ellipse extends beyond the bounds of the plot and is indeed elliptical. It can be seen that the true transmitter location does not correspond to a location with minimal error, suggesting that modeling errors are present.

## 7. CONCLUSIONS

A novel method for geolocation of a circularly scanning radar transmitter based on observing times between detection of a distributed set of receivers was introduced. This method has the benefits of minimum complexity and minimal timing requirements. This, in turn, enables the technology to be used on a variety of platforms in a multitude of configurations without the need for precise timing calibration or high data

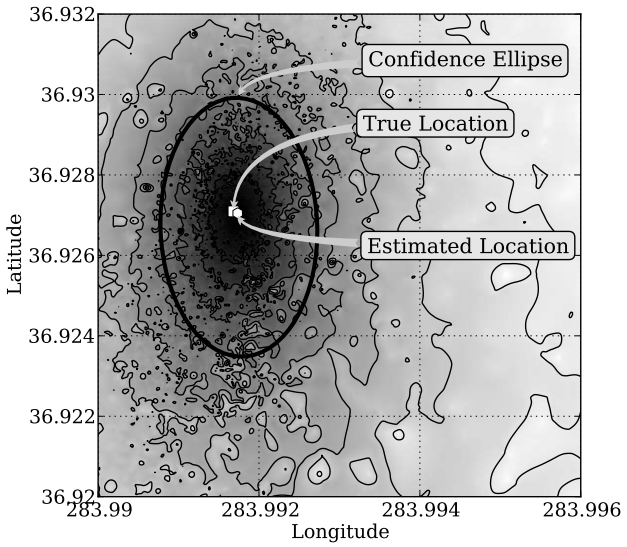


**Figure 4**. Plot Showing Nonlinear Analysis Results for Dataset F1 with Error Contours

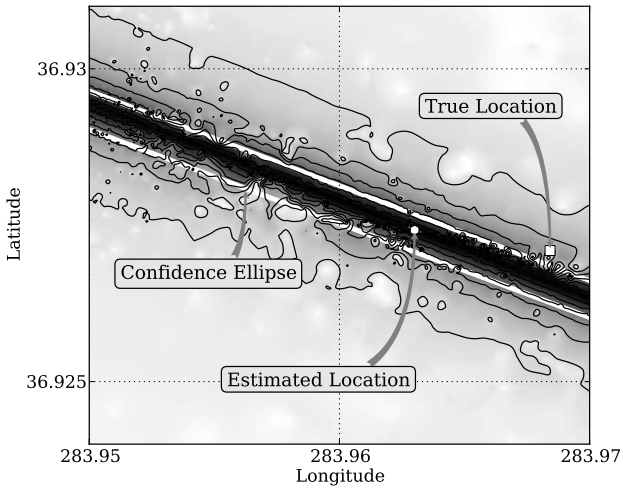


**Figure 5**. Plot Showing Nonlinear Analysis Results for Dataset F3 with Error Contours

transfer rates. Both linear and nonlinear methods were explored for solving this system. Using a particle swarm optimizer enabled precise geolocation, while being tolerant of the nonlinearities of the solution space. An analysis of the confidence region associated with the solution showed that the uncertainty in the position of solution for the radar transmitter is relatively small; however, it also suggests that modeling improvements may be made.

With this in mind, future work includes incorporating a scan rate drift term in the estimation process. This requires relatively low effort for implementation in the PSO and will allow a more accurate result given a non-constant scan rate. In addition, incorporating angle of arrival (AOA) information within the estimation process should increase the accuracy of the results while maintaining minimal complexity. Uncertainty in AOA measurements are generally orthogonal to the uncertainty in the DCTOA measurement. This should allow for increased accuracy.

Ultimately, the technology shows enormous potential in a variety of fields. The future of some fields, such as maritime domain awareness, are dependent upon the use of a network of disparate sensors. This method will enable these sensors to perform precision radar geolocation without the need for expensive precision timing calibration and high data transfer rates.

## APPENDIX

The partial derivatives of the nonlinear measurement given in Equation 1 may be calculated as follows. Consider the following system.

$$\boldsymbol{x} = \begin{bmatrix} \boldsymbol{r} \\ \omega \end{bmatrix} \tag{29}$$

$$\boldsymbol{y} = \frac{1}{\omega} \cos^{-1}\left( \frac{(\boldsymbol{r}_1 - \boldsymbol{r}) \cdot (\boldsymbol{r}_2 - \boldsymbol{r})}{|\boldsymbol{r}_1 - \boldsymbol{r}|\,|\boldsymbol{r}_2 - \boldsymbol{r}|} \right) \tag{30}$$

$$\tag{31}$$

Now assume that positions are restricted to the local tangent plane and let $\boldsymbol{\rho}_i = \boldsymbol{r}_i - \boldsymbol{r}$. So then, the following are true.

$$\boldsymbol{x} = \begin{bmatrix} x \\ y \\ \omega \end{bmatrix} \tag{32}$$

$$\boldsymbol{y} = \frac{1}{\omega} \cos^{-1}\left( \frac{(\boldsymbol{\rho}_1) \cdot (\boldsymbol{\rho}_2)}{|\boldsymbol{\rho}_1|\,|\boldsymbol{\rho}_2|} \right) \tag{33}$$

$$\tag{34}$$

So then the partial derivatives of $h$ with respect to the first position state, $x$ is as follows.

$$\frac{\partial h}{\partial x} = \mp \frac{1}{\omega\sqrt{1-\gamma^2}} \frac{\partial u}{\partial x} \tag{35}$$

$$\gamma = \frac{\boldsymbol{\rho}_1 \cdot \boldsymbol{\rho}_2}{|\boldsymbol{\rho}_1|\,|\boldsymbol{\rho}_2|} \tag{36}$$

$$\frac{\partial u}{\partial x} = \frac{-\rho_1(1) - \rho_2(1)}{|\boldsymbol{\rho}_1|\,|\boldsymbol{\rho}_2|} \tag{37}$$

$$+ \rho_1(1) \frac{\boldsymbol{\rho}_1 \cdot \boldsymbol{\rho}_2}{|\boldsymbol{\rho}_1|^3\,|\boldsymbol{\rho}_2|} \tag{38}$$

$$+ \rho_2(1) \frac{\boldsymbol{\rho}_1 \cdot \boldsymbol{\rho}_2}{|\boldsymbol{\rho}_1|\,|\boldsymbol{\rho}_2|^3} \tag{39}$$

Here, $\boldsymbol{\rho}(i)$ represents the $i^{th}$ component of $\boldsymbol{\rho}$ vector. The partial derivative of $h$ with respect to the second position state, $y$, is as follows

$$\frac{\partial h}{\partial y} = \mp \frac{1}{\omega\sqrt{1-\gamma^2}} \frac{\partial u}{\partial y} \tag{40}$$

$$\frac{\partial u}{\partial y} = \frac{-\rho_1(2) - \rho_2(2)}{|\boldsymbol{\rho}_1|\,|\boldsymbol{\rho}_2|} \tag{41}$$

$$+ \rho_1(2) \frac{\boldsymbol{\rho}_1 \cdot \boldsymbol{\rho}_2}{|\boldsymbol{\rho}_1|^3\,|\boldsymbol{\rho}_2|} \tag{42}$$

$$+ \rho_2(2) \frac{\boldsymbol{\rho}_1 \cdot \boldsymbol{\rho}_2}{|\boldsymbol{\rho}_1|\,|\boldsymbol{\rho}_2|^3} \tag{43}$$

Finally, the partial derivative of $h$ with respect to the scan rate, $\omega$, is as follows.

$$\frac{\partial h}{\partial \omega} = \mp \frac{1}{\omega^2} \arccos\left( \frac{\boldsymbol{\rho}_1 \cdot \boldsymbol{\rho}_2}{|\boldsymbol{\rho}_1|\,|\boldsymbol{\rho}_2|} \right) \tag{44}$$

The sign ambiguity on these terms is related to the ambiguity presented in Equation 4. The partial derivatives are negative for the case where the radar has swept through $\theta$ or $2\pi + \theta$, while the partial derivatives are positive for the case where the radar has swept out $2\pi - \theta$.

## REFERENCES


[1] D. Koks, "Numerical calculations for passive geolocation scenarios," Defense Science and Technology Organisation, Edinburgh, SA 5111, Australia, Tech. Rep. DSTO-RR-0319, 2007.

[2] R. Wiley, *Electronic intelligence: the analysis of radar signals*, ser. The Artech House radar library. Artech House, 1993.

[3] D. Torrieri, "Statistical theory of passive location systems," *Aerospace and Electronic Systems, IEEE Transactions on*, vol. AES-20, no. 2, pp. 183 –198, march 1984.

[4] B. Lee, Y. Chan, F. Chan, H.-J. Du, and F. A. Dilkes, "Doppler frequency geolocation of uncooperative radars," in *Military Communications Conference, 2007. MILCOM 2007. IEEE*, Oct. 2007, pp. 1 –6.

[5] R. Stansfield, "Statistical theory of d.f. fixing," *Electrical Engineers - Part IIIA: Radiocommunication, Journal of the Institution of*, vol. 94, no. 15, pp. 762 –770, march-april 1947.

[6] H. Hmam, "Scan-based emitter passive localization," *IEEE Transactions on Aerospace and Electronic Systems*, vol. 43, no. 1, pp. 36–54, January 2007.

[7] H. Hmam and K. Doğançay, "Joint estimation of scan rate and emitter location in scan based passive localization systems," in $15^{th}$ *European Signal Processing Conference*. Poznań, Poland: EURASIP, 2007.

[8] H. Hmam, "Passive localization of scanning emitters," *IEEE Transactions on Aerospace and Electronic Systems*, vol. 46, no. 2, pp. 944–951, April 2010.

[9] C. T. Powell, G. M. Nichols, M. S. Hurley, J. W. Middour, L. V. Geluso, and D. A. Hayes, "Sea-node and searchlight results achieved during trident warrior-09," Naval Research Laboratory, Washington, DC 20375-5320, Tech. Rep. NRL/FR/5720–10-10,202, 2010.

[10] J. Middour, K. Bynum, C. Huffine, A. D'Agostino, C. Chrisman, C. Ellis, and R. Nichols, "Method and apparatus for passively locating radar emissions from rotating transmitters," U.S. Patent US 7,952,523 B2, May 31, 2011.

[11] B. D. Tapley, B. E. Schutz, and G. H. Born, *Statistical Orbit Determination*. Elsevier Academic Press, 2004.

[12] C. Lawson and R. Hanson, *Solving Least Squares Problems*. Prentice-Hall, Inc., 1974.

[13] J. Kennedy and R. Eberhart, "Particle swarm optimization," in *Proc. IEEE International Conf. on Neural Networks (Perth, Australia)*. IEEE Service Center, 1995.

[14] R. Eberhart and J. Kennedy, "A new optimizer using particle swarm theory," in *Proc. of the Sixth International Symposium on Micromachine and Human Learning (Nagoya, Japan)*, 1995.

[15] J. Kennedy and R. C. Eberhart, *Swarm Intelligence*. Elsevier Academic Press, 2001.

[16] S. Das, A. Abraham, and A. Konar, "Particle swarm optimization and differential evolution algorithms: Technical analysis, applications and hybridization perspectives," in *Advances of Computational Intelligence in Industrial Systems*, ser. Studies in Computational Intelligence, Y. Liu, A. Sun, H. Loh, W. Lu, and E.-P. Lim, Eds. Springer, 2008, vol. 116, pp. 1–38.

[17] J. Kennedy, "Small worlds and mega-minds: effects of neighborhood topology on particle swarm performance," in *Evolutionary Computation, 1999. CEC 99. Proceedings of the 1999 Congress on*, vol. 3, 1999.

[18] E. Ozcan and C. Mohan, "Particle swarm optimization: surfing the waves," in *Evolutionary Computation, 1999. CEC 99. Proceedings of the 1999 Congress on*, vol. 3, 1999, pp. 3 vol. (xxxvii+2348).

[19] I. C. Trelea, "The particle swarm optimization algorithm: convergence analysis and parameter selection," *Information Processing Letters*, vol. 85, no. 6, pp. 317 – 325, 2003.

[20] P. R. Wolf and C. D. Ghilani, *Adjustment Computations: Spatial Data Analysis*, 4th ed. John Wiley and Sons, Inc, 2006.

[21] M. Schwaab, E. C. Biscaia, J. L. Monteiro, and J. C. Pinto, "Nonlinear parameter estimation through particle swarm optimization," *Chemical Engineering Science*, vol. 63, no. 6, pp. 1542–1552, March 2008.

[22] J. R. Donaldson and R. B. Schnabel, "Computational experience with confidence regions and confidence intervals for nonlinear least squares," *Technometrics*, vol. 29, no. 1, pp. 67–82, Feb 1987.

[23] E. M. L. Beale, "Confidence regions in non-linear estimation," *Journal of the Royal Statistical Society. Series B (Methodological)*, vol. 22, no. 1, pp. pp. 41–88, 1960.


## BIOGRAPHY

**John G. Warner** focuses his expertise to solve problems relating to astrodynamics and nonlinear estimation. He joined the US Naval Research Laboratory last year as a Karle's Fellow fresh from receiving MS and BS degrees in aerospace engineering from the University of Illinois at Urbana-Champaign. While at NRL he has lead efforts to improve atmospheric modeling within orbit determination software and has applied nonlinear optimization techniques to solve a range of problems.

**Jay W. Middour** has more than twenty-five years experience doing space systems research and development. He is presently the head of the Space Systems Technology Branch at the Naval Research Laboratory in Washington, DC, and is the former head of the NRL Astrodynamics Office. Mr. Middour leads a broad range of investigations and projects including Radio Frequency and Optical Space Payloads, Satellite Laser Ranging, Signal Processing, Calibration, and Space Navigation Systems.